

# GlimpRouter: Efficient Collaborative Inference by Glimpsing One Token of Thoughts

Anonymous ACL submission

## Abstract

Large Reasoning Models (LRMs) achieve remarkable performance by explicitly generating multi-step chains of thought, but this capability incurs substantial inference latency and computational cost. Collaborative inference offers a promising solution by selectively allocating work between lightweight and large models, yet a fundamental challenge remains: determining when a reasoning step requires the capacity of a large model or the efficiency of a small model. Existing routing strategies either rely on local token probabilities or post-hoc verification, introducing significant inference overhead. In this work, we propose a novel perspective on step-wise collaboration: the difficulty of a reasoning step can be inferred from its very first token. Inspired by the “Aha Moment” phenomenon in LRMs, we show that the entropy of the initial token serves as a strong predictor of step difficulty. Building on this insight, we introduce GlimpRouter, a training-free step-wise collaboration framework. GlimpRouter employs a lightweight model to generate only the first token of each reasoning step and routes the step to a larger model only when the initial token entropy exceeds a threshold. Experiments on multiple benchmarks demonstrate that our approach significantly reduces inference latency while preserving accuracy. For instance, GlimpRouter attains a substantial 10.7% improvement in accuracy while reducing inference latency by 25.9% compared to a standalone large model on AIME25. These results suggest a simple yet effective mechanism for reasoning: allocating computation based on a glimpse of thought rather than full-step evaluation.

## 1 Introduction

Large reasoning models, such as DeepSeek-R1 (Guo et al., 2025) and OpenAI o1/o3 (Jaeck et al., 2024; OpenAI, 2025), have demonstrated remarkable performance across a wide range of com-

plex reasoning tasks by explicitly generating structured reasoning steps (Yang et al., 2025c; Wang et al., 2025b,a; Chen et al., 2025a; Li et al., 2025; Hu et al., 2025). However, this capability comes at a high cost: extended reasoning chains inevitably incur high inference latency and substantial computational overhead, severely limiting the practicality of LRMs in latency-sensitive and resource-constrained settings.

To alleviate this bottleneck, collaborative inference has emerged as a promising paradigm (She et al., 2025; Xiao et al., 2025; Qu et al., 2025). The key idea is that multiple models with heterogeneous capabilities and costs are orchestrated to jointly solve a task: lightweight models handle routine or easy tasks, while more powerful but expensive models are invoked selectively for difficult ones (Chen et al., 2025b; Wang et al., 2025d). Existing collaboration strategies generally fall into two categories. Token-level methods, such as Speculative Decoding (Leviathan et al., 2023; Fu et al., 2025), accelerate generation by allowing a small model to propose candidate tokens that are then verified (and possibly accepted) by a larger model, reducing the number of expensive forward passes. In contrast, step-level methods attempt to route entire reasoning steps between models. They typically depend on *post-hoc* verification, such as LLM-as-a-judge (Shi et al., 2025; Pan et al., 2025), or on averaged uncertainty metrics (e.g., mean perplexity or entropy) (Cui et al., 2025; Zhang et al., 2025).

Despite their promise, determining the optimal allocation of tasks between large and small models remains a fundamental challenge. Token-level methods rely primarily on local token probabilities and frequently switch models at a fine granularity, while step-level strategies require evaluating entire reasoning steps before making routing decisions. Both approaches introduce non-trivial computational overhead, which can partially or even fully offset their intended efficiency gains.

In this work, we advance a new perspective: *Can we judge the difficulty of a reasoning step at the very beginning?* Inspired by the “Aha Moment” phenomenon observed in LRMs (Guo et al., 2025), previous works suggest that the onset of a reasoning step—often marked by discourse cues such as “Wait”, “But”, or “So”—represents a cognitive pivot that shapes the entire subsequent reasoning trajectory (Wang et al., 2025c; Yang et al., 2025b; Zeng et al., 2025b). We hypothesize that the information associated with this *initial token* provides a more discriminative signal of step-level difficulty than averaged statistics over the full step. To validate this hypothesis, we analyze the uncertainty distribution of the reasoning steps across various tasks (Section 2). The experimental results show that the entropy of the initial tokens exhibits an exceptionally high variance, indicating it is a powerful discriminator: steps with low initial entropy typically correspond to routine derivations that a small model can readily process, whereas steps with high initial entropy indicate critical cognitive bifurcations that require the collaboration of larger, more powerful models.

Building on this insight, we propose **GlimpRouter**, a novel training-free framework for efficient collaborative inference. At each reasoning step, a lightweight model is first used to generate only the initial token of the step. If the entropy of this token falls below a predefined threshold, the lightweight model proceeds to generate the entire step; otherwise, the generated context is seamlessly handed over to a larger and more capable model. In effect, this mechanism essentially operationalizes the principle of “*A Glimpse of Thought*”: a minimal signal from the onset of a reasoning step governs the computational budget allocated to its full generation.

We empirically evaluate our approach on a diverse set of reasoning benchmarks, including mathematical reasoning (AIME), challenging general reasoning (GPQA (Rein et al., 2024)), and code generation (LiveCodeBench (Jain et al., 2024)). Across all benchmarks, GlimpRouter achieves a superior trade-off between efficiency and performance. For instance, on the AIME25 benchmark, our method attains a substantial **10.7%** improvement in accuracy while simultaneously reducing inference latency by **25.9%** compared to a standalone large model. Moreover, we demonstrate that our step-level routing strategy is orthogonal to

token-level speculative decoding, enabling complementary and compound speedups when integrated. Our contributions are summarized as follows:

- We perform an analysis of the uncertainty distribution across reasoning steps and identify that the entropy of the initial token serves as an indicator of reasoning difficulty.
- We propose **GlimpRouter**, a simple yet effective mechanism that enables training-free, step-aware collaboration between models.
- Extensive experiments verify that our method significantly reduces latency while maintaining or even enhancing the reasoning efficacy of large models, offering a practical solution for deploying efficient LRMs.

## 2 A Preliminary Study

Previous works have suggested that the onset of a reasoning step—often marked by discourse cues such as “Wait”, “But”, or “So”—represents a cognitive pivot that shapes the entire subsequent reasoning trajectory (Wang et al., 2025c; Yang et al., 2025b; Zeng et al., 2025b). Building on this intuition, we hypothesize that the uncertainty associated with the *initial token* of a reasoning step provides a more discriminative signal of step-level difficulty than statistics aggregated over the full step. In other words, the essential difficulty information is concentrated at the very beginning of each reasoning step. In this section, we analyze the uncertainty distribution for the reasoning steps and examine how different uncertainty metrics correlate with step-wise difficulty.

### 2.1 Study Design

To quantify uncertainty within a reasoning step, we analyze entropy-based metrics derived from the model’s conditional probability distribution  $P_\theta$ . It is well-established that the internal logits of LLMs serve as a reliable proxy for model confidence (Mallin and Gales, 2020; Kuhn et al., 2023). Let  $s_k = \{t_1, \dots, t_L\}$  denote the  $k$ -th reasoning step with  $L$  tokens, and  $\mathbf{c}_k$  be the preceding context of this step.

**Step Entropy ( $\mathbf{H}_{\text{step}}$ ).**  $\mathbf{H}_{\text{step}}$  quantifies the average uncertainty across all tokens in a reasoning step:

$$\mathbf{H}_{\text{step}}(s_k) = \frac{1}{L} \sum_{i=1}^L \mathbf{H}(P_\theta(\cdot | t_{<i}, \mathbf{c}_k)) \quad (1)$$

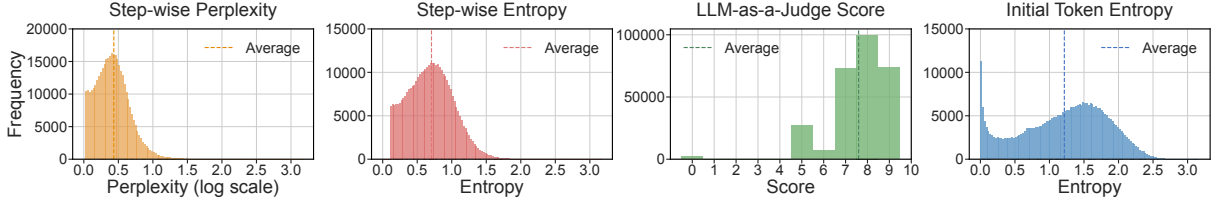


Figure 1: Comparison of the distributions of different uncertainty metrics. Unlike other metrics, which exhibit a generic unimodal distribution, the entropy of initial thought tokens ( $\mathbf{H}_{\text{init}}$ ) displays a distinct bimodal and heavy-tailed distribution. This indicates that  $\mathbf{H}_{\text{init}}$  serves as a discriminative signal, effectively capturing the ‘‘Aha Moments’’ that distinguish complex reasoning steps from routine derivations.

where  $\mathbf{H}(p) = -\sum_{v \in V} p(v) \log p(v)$  denotes the Shannon entropy of a distribution (Shannon, 1948). This metric treats all tokens within the step uniformly by averaging uncertainty across the entire sequence.

**Initial Token Entropy ( $\mathbf{H}_{\text{init}}$ ).** In contrast,  $\mathbf{H}_{\text{init}}$  captures the uncertainty of the *initial token* for each step:

$$\mathbf{H}_{\text{init}}(s_k) = \mathbf{H}(P_{\theta}(t_1 | \mathbf{c}_k)) \quad (2)$$

Unlike step-level averages,  $\mathbf{H}_{\text{init}}$  isolates the uncertainty at the onset of the step, which we hypothesize to be an indicator of the step’s difficulty.

As additional baselines, we consider the following commonly used metrics in collaborative inference.

**Step-wise Perplexity ( $\text{PPL}_{\text{step}}$ ).**  $\text{PPL}_{\text{step}}$  measures the exponentiated average negative log-likelihood over the entire step:

$$\text{PPL}_{\text{step}}(s_k) = \exp \left( -\frac{1}{L} \sum_{i=1}^L \log P_{\theta}(t_i | t_{<i}, \mathbf{c}_k) \right) \quad (3)$$

Like  $\mathbf{H}_{\text{step}}$ ,  $\text{PPL}_{\text{step}}$  aggregates uncertainty uniformly across all tokens.

**LLM-as-a-Judge.** It assesses the validity of a reasoning step using the large model directly. Given a step  $s_k$  and its context  $\mathbf{c}_k$ , the LLM assigns a scalar score  $S \in \{0, 1, \dots, 9\}$ . We note that this metric requires an additional computationally expensive inference pass and is therefore unsuitable for efficiency-critical routing decisions.

We examine the reasoning traces using Qwen3-4B, Qwen3-32B (Yang et al., 2025a), and DeepSeek-R1-Distill-Qwen-32B (Guo et al., 2025) on the AIME and LiveCodeBench datasets (Jain et al., 2024), collecting over 10 million tokens of reasoning steps.

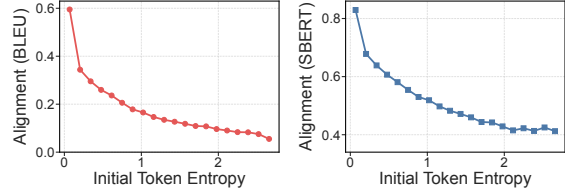


Figure 2: Alignment between the outputs generated by small and large models under various  $\mathbf{H}_{\text{init}}$  intervals.

## 2.2 Results and Analysis

### Information Distribution within Reasoning Steps.

Figure 1 illustrates the distributions reflected by the four metrics. It is evident that both  $\text{PPL}_{\text{step}}$  and  $\mathbf{H}_{\text{step}}$  exhibit narrow, unimodal distributions clustered around central values. We attribute this to the *signal dilution* effect: a reasoning step typically contains a few critical decision tokens followed by a long sequence of deterministic syntactic tokens. Averaging over the entire step smooths out the local spikes of uncertainty, making these metrics insensitive to the actual difficulty. Similarly, the LLM-as-a-Judge distribution is discrete and highly skewed towards high scores (saturation), lacking the granularity required for fine-grained routing thresholds. In contrast,  $\mathbf{H}_{\text{init}}$  presents a distinct bimodal distribution with a heavy tail. The clear separation between the low-entropy peak (routine steps) and the high-entropy tail (complex reasoning) suggests that  $\mathbf{H}_{\text{init}}$  naturally functions as a high-sensitivity discriminator for routing.

**Correlations to Model Routing.** Motivated by the observation that most information in a reasoning step resides at its onset, we further examine whether this signal can serve as an indicator for model routing, where a lightweight language model can reliably substitute a large model. To this end, we partition reasoning steps into intervals based on  $\mathbf{H}_{\text{init}}$  predicted by the small model. For each interval, we evaluate the alignment between the outputs generated by the small and large models,

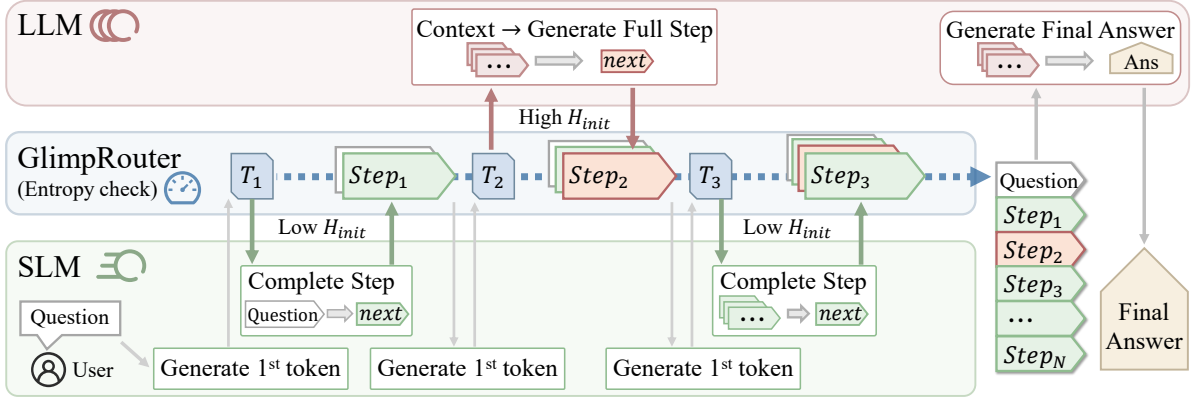


Figure 3: The overall framework of **GlimpRouter**. The collaborative inference pipeline operates in a step-wise manner. At the onset of each reasoning step, the SLM first generates a “glimpse” (the initial token  $T_k$ ). GlimpRouter then computes the entropy  $H_{init}$  of this token to gauge step difficulty. Based on the threshold, the system dynamically routes the generation: (1) Delegate (Low  $H_{init}$ ): Routine steps are fully generated by the efficient SLM. (2) Intervene (High  $H_{init}$ ): Complex steps signaling cognitive pivots are routed to the capable LLM for robust reasoning. Finally, the LLM generates the conclusive answer based on the aggregated collaborative chain.

249 conditioned on the same preceding context  $c$ . We  
 250 quantify alignment using two widely used similar-  
 251 ity metrics: BLEU-4 (Lin and Och, 2004), which  
 252 captures lexical overlap, and SBERT (Reimers and  
 253 Gurevych, 2019), which measures semantic simi-  
 254 larity. As shown in Figure 2, we observe a strictly  
 255 monotonic negative correlation between  $H_{init}$  and  
 256 both similarity metrics. In the low- $H_{init}$  regime,  
 257 the small model’s outputs closely align with those  
 258 of the large model, indicating that such steps can  
 259 be handled competently by the lightweight model.  
 260 In contrast, as  $H_{init}$  increases, the alignment de-  
 261 grades substantially, reflecting growing divergence  
 262 in both surface form and semantic content. This  
 263 strong correlation provides empirical evidence that  
 264  $H_{init}$  can be a reliable predictor of step-level dif-  
 265 ficulty, thereby suggesting a routing strategy in  
 266 which a small model can substitute a large model  
 267 in low- $H_{init}$  steps without compromising results.  
 268 To provide concrete intuition for this correlation,  
 269 we present qualitative case studies in Appendix F.

### 270 3 Methodology

#### 271 3.1 Problem Formulation

272 We consider a collaborative inference framework  
 273 involving a large, high-capacity reasoning model  
 274 (LLM,  $M_L$ ) and a small computationally efficient  
 275 model (SLM,  $M_S$ ). Large reasoning models typi-  
 276 cally output a reasoning process  $\mathcal{T}$ , often encapsu-  
 277 lated within a `<think>...</think>` tag, followed  
 278 by the final answer  $A$ . Our framework focuses  
 279 on accelerating the reasoning process  $\mathcal{T}$ , while  
 280 the final answer  $A$  is always generated by  $M_L$

281 to ensure correctness. Formally, the reasoning  
 282 process is decomposed into a sequence of steps  
 283  $\mathcal{T} = \{s_1, \dots, s_K\}$  based on structural delimiters  
 284 (e.g., double newlines (Pan et al., 2025; Yang et al.,  
 285 2025b)). Each step  $s_k$  consists of a sequence of  
 286 tokens  $s_k = (t_1, \dots, t_L)$  and is generated con-  
 287 ditioned on the preceding context  $c_k$ , which includes  
 288 the original question and all previous generated  
 289 steps  $s_1, \dots, s_{k-1}$ . The objective of collaborative  
 290 inference is to dynamically assign each reasoning  
 291 step  $s_k$  to  $M_S$  or  $M_L$ , minimizing overall inference  
 292 latency while preserving the quality of reasoning  
 293 required for accurate solutions.

#### 294 3.2 Overview

295 To navigate the efficiency-accuracy trade-off, we  
 296 propose **GlimpRouter**, a training-free, step-aware  
 297 collaboration strategy that routes reasoning steps  
 298 based on the *initial token entropy* ( $H_{init}$ ). Figure 3  
 299 illustrates the overall pipeline. Given an input ques-  
 300 tion, the system operates in a step-wise manner.  
 301 At the onset of each step, instead of blindly gener-  
 302 ating the full content, GlimpRouter employs  $M_S$   
 303 to “glimpse” the first token, yielding an entropy  
 304  $H_{init}$  that quantizes the difficulty of the upcoming  
 305 step: If  $H_{init}$  falls below a threshold, the step is  
 306 deemed routine, and the small model is responsi-  
 307 ble for continuing the generation. Otherwise, the  
 308 step signals a cognitive pivot, and the context is  
 309 handed over to a large model for high-quality gen-  
 310 eration. This “Probe-then-Dispatch” mechanism  
 311 ensures that heavy computational resources are al-  
 312 located solely for critical reasoning steps. Each

step is introduced in the following sections. The detailed procedure is outlined in Algorithm 1 in Appendix A.

### 3.3 Glimpse: Initial Token Probing

At the beginning of the reasoning step  $k$ , given the preceding context  $c_k$ , the small model  $M_S$  is invoked to predict the probability distribution of only the first token  $t_{k,1}$ . We compute the entropy  $\mathbf{H}_{\text{init}}(s_k)$  of this distribution as a proxy for the cognitive uncertainty of the current reasoning step. This probing operation incurs a marginal computational cost equivalent to decoding a single token, unlike methods that necessitate generating an entire reasoning step (typically  $L \gg 1$  tokens) before verification. Even in scenarios where the step is subsequently identified as difficult and routed to  $M_L$  (thereby discarding the probe), this 1-token overhead is negligible compared to the substantial sunk costs associated with discarding fully generated invalid steps.

### 3.4 Dynamic Model Routing

Given the entropy of the initial token in the current step, GlimpRouter dispatches the generation task to the appropriate model based on a threshold  $\tau$ : **Delegate** ( $\mathbf{H}_{\text{init}}(s_k) \leq \tau$ ): Low entropy suggests that the small model is confident in the logical progression, and the step is likely routine. Consequently,  $M_S$  continues to autoregressively generate the remainder of step  $s_k$  until the delimiter is reached. This decision reduces the total cost by maximizing the utilization of the small model.

**Intervene** ( $\mathbf{H}_{\text{init}}(s_k) > \tau$ ): High entropy indicates logical ambiguity or high cognitive load. In this scenario,  $M_L$  is selected to generate the step  $s_k$ . While this incurs a higher computational cost, it leverages the superior reasoning and inherent self-correction capabilities of LRMs (Guo et al., 2025). Specifically,  $M_L$  can rectify potential logical drifts accumulated in the historical context  $c_k$ , thereby satisfying the quality constraint. We provide a qualitative analysis of this implicit self-correction behavior in Appendix F.

### 3.5 Efficient Model Switching

A critical requirement for a step-level collaboration system, where every step involves context transitions, is minimizing the model switching overhead. To minimize the system overhead, we leverage prefix caching mechanisms supported by inference engines (Kwon et al., 2023; Zheng et al., 2024).

When routing a request between models, the context  $c_k$ , which comprises the question and historical steps, is largely resident in the KV cache from previous interactions. Thus, the context processing is reduced to a highly parallelizable prefill phase rather than a serial re-computation. The resulting switching latency is comparable to decoding a few tokens, ensuring that the computational savings from  $M_S$  are not negated by routing overheads.

### 3.6 Hierarchical Acceleration

A distinct advantage of GlimpRouter lies in its step-level granularity. This coarse-grained design is inherently orthogonal to token-level optimizations, allowing our framework to be seamlessly integrated with various low-level acceleration techniques to achieve compound speedups. To maximize system throughput, we implement a hierarchical acceleration strategy in Section 4.3. At the inter-step level, GlimpRouter acts as a global planner, assigning routine logical steps to  $M_S$  to bypass the expensive  $M_L$  entirely. At the intra-step level, when  $M_L$  is invoked, we further accelerate its generation using Speculative Decoding (Leviathan et al., 2023). Specifically, we employ a ‘‘Draft-then-Verify’’ pipeline where the small draft model  $M_S$  proposes token sequences that are verified in parallel by  $M_L$ .

## 4 Experiments

### 4.1 Experimental Setup

**Models and Configurations.** We conduct comprehensive experiments using the Qwen3 (Yang et al., 2025a) and DeepSeek-R1 (Guo et al., 2025) families. We utilize Qwen3-4B as the small model (SLM) and DeepSeek-R1-Distill-Qwen-32B as the large model (LLM). This setup serves as the default configuration for our results. To verify the scalability of GlimpRouter, we extend our analysis to Qwen3-32B as the LLM in Section 4.2 and DeepSeek-R1-Distill-Qwen-1.5B as the SLM in Appendix B, covering a spectrum of model sizes and architectural pairings.

**Benchmarks.** We evaluate our method on a diverse set of complex reasoning tasks. For mathematical reasoning, we employ AIME24 and AIME25, which represent the frontier of mathematical problem-solving. For general reasoning, we use GPQA-Diamond (Rein et al., 2024), an expert-written, challenging multiple-choice dataset

LLM	Method	AIME24		AIME25		GPQA		LCBv5		LCBv6	
		Acc ↑	Lat ↓	Acc ↑	Lat ↓	Acc ↑	Lat ↓	Acc ↑	Lat ↓	Acc ↑	Lat ↓
-	SLM only	48.33	99	45.00	105	61.11	76	47.90	100	43.71	94
Qwen3-32B	LLM only	60.00	220	48.33	231	61.87	194	<b>52.69</b>	249	<b>47.43</b>	241
	Random	56.67	134	47.50	136	61.74	128	51.20	147	44.00	146
	RSD	59.17	167	47.50	173	62.50	165	51.05	209	46.29	208
	SpecCoT	58.33	161	48.33	170	61.62	163	51.05	195	45.71	192
	SpecReason	60.00	160	49.17	162	62.63	181	51.50	213	46.29	214
	GlimpRouter	<b>60.83</b>	145	<b>51.67</b>	147	<b>63.01</b>	142	<b>52.69</b>	162	47.14	165
DeepSeek-32B	LLM only	57.50	197	46.67	220	61.62	176	52.40	219	46.86	214
	Random	56.67	137	48.33	147	62.50	114	52.25	142	47.00	131
	RSD	58.33	167	45.83	171	63.64	146	51.95	180	45.71	178
	SpecCoT	60.00	159	50.00	175	62.75	135	53.29	168	47.14	165
	SpecReason	57.50	158	49.17	169	63.76	213	53.59	185	47.57	189
	GlimpRouter	<b>60.83</b>	143	<b>51.67</b>	163	<b>64.02</b>	129	<b>54.64</b>	160	<b>48.29</b>	160

Table 1: Performance comparison with Qwen3-32B and DeepSeek-R1-Distill-Qwen-32B as LLM, and SLM is fixed as Qwen3-4B. Acc and Lat represent Accuracy (Pass@1, %) and Average Latency (s), respectively. The best performance within each group is highlighted in bold.

in biology, physics, and chemistry. For code generation, we utilize LiveCodeBench (v5 and v6) (Jain et al., 2024), which evaluates the model’s ability to solve competitive programming problems.

**Baselines.** We compare GlimpRouter against standalone models and state-of-the-art collaborative inference baselines. **Standalone SLM / LLM:** The individual performance of the small and large models, serving as the efficiency and performance boundaries, respectively. **Random:** A method using a random score from 0 to 9 to select the model for inference. **RSD (Liao et al., 2025):** A reward-guided method that employs a trained Process Reward Model (PRM) to evaluate the quality of the step and determine whether to invoke the large model. **SpecCoT (Shi et al., 2025):** A selection-based collaboration method where the small model generates multiple candidate reasoning steps in parallel. The large model acts as a discriminator to select the optimal step. **SpecReason (Pan et al., 2025):** A verification-based method where the small model generates a step, which is then verified by the large model acting as a judge. Upon rejection, the large model falls back to generation.

**Metrics.** We assess the efficiency-performance trade-off using two key metrics. **Pass@1 (Acc):** The percentage of problems solved correctly on the first attempt. **Latency (Lat):** The end-to-end wall-clock time (in seconds) per question, serving

as the primary indicator of inference efficiency.

**Implementation Details.** All experiments are conducted on NVIDIA A100-80GB GPUs using the vLLM inference engine (Kwon et al., 2023). We employ sampling with a temperature of 0.6 and a top-p of 0.95. The maximum budget for reasoning tokens is set to 8192. For the hierarchical acceleration strategy, we repurpose the SLM to serve as the token-level drafter for the LLM with a draft length of  $n = 3$ . To ensure statistical stability, all reported results are averaged over 4 runs. Regarding the entropy threshold  $\tau$ , since it modulates the trade-off between latency and accuracy, we report the configuration that achieves the optimal balance, maximizing accuracy while securing significant latency reduction, in our main results. Empirically, this corresponds to an *intervention rate* (percentage of steps generated by LLM) of approximately 20%–30%. A detailed sensitivity analysis of  $\tau$  is provided in Section 4.3.

## 4.2 Main Results

Table 1 presents the comparative performance of GlimpRouter against baselines on five complex reasoning benchmarks. GlimpRouter consistently achieves the optimal trade-off between inference latency and reasoning accuracy across different model configurations. In the primary setting using Qwen3-4B as the SLM, our method consistently outperforms the standalone LLM (DeepSeek-R1-

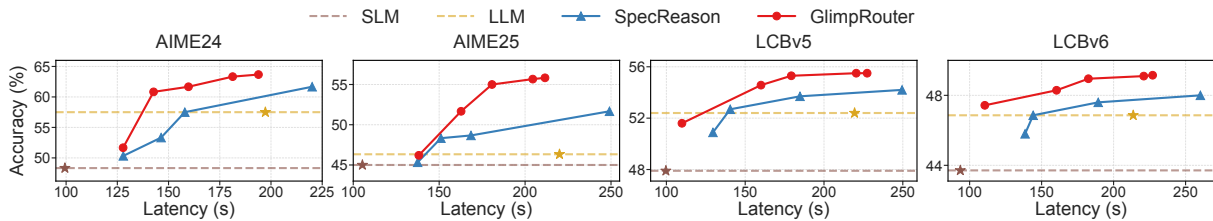


Figure 4: Sensitivity analysis of collaboration threshold on multiple benchmarks. GlimpRouter (red circles) establishes a superior Pareto frontier compared to the SpecReason (blue triangles). Dashed lines represent the performance of standalone models.

Distill-Qwen-32B) in accuracy while delivering substantial speedups. Specifically, GlimpRouter reduces end-to-end latency by **25.2%–27.4%** across all datasets compared to the LLM-only baseline. For instance, on AIME25, we observe a substantial **10.7%** relative improvement in accuracy combined with a **25.9%** reduction in latency.

Compared to existing step-level collaboration methods, GlimpRouter demonstrates a distinct advantage in efficiency. While baselines like RSD, SpecCoT, and SpecReason achieve better accuracy than the SLM-only baseline, they still incur significant latency overheads. For example, SpecReason’s latency on GPQA (213s) exceeds even that of the standalone LLM, DeepSeek-R1-Distill-Qwen-32B (176s), negating the benefits of collaboration. This inefficiency stems from their routing mechanisms: all methods require generating full reasoning steps (and often multiple candidates) or performing post-hoc verification before making a decision. In contrast, GlimpRouter determines the routing path based solely on the *initial token entropy*. This “Probe-then-Dispatch” mechanism minimizes the computational overhead of the decision process.

A counterintuitive yet compelling result is that our collaborative framework outperforms the accuracy of the standalone large model (e.g., 51.67% vs. 46.67% on AIME25). We attribute this to the self-correction capacity of LRMs (Guo et al., 2025; Zeng et al., 2025a). The intervention mechanism in our framework offers more than just text completion. The high entropy at the onset of a step often serves as a manifestation of latent inconsistencies accumulated in the preceding trajectory. When GlimpRouter detects this uncertainty and invokes the LLM, the large model does not merely continue the sequence; effective intervention allows it to implicitly re-evaluate the context and rectify prior logical drifts, thereby realigning the reasoning path. We provide concrete case studies illustrating this correction behavior in Appendix F.

### 4.3 Ablation and Analysis

**Sensitivity Analysis of Collaboration Threshold.** The trade-off between inference efficiency and reasoning capability is closely associated with the proportion of steps routed to the large model, referred to as the *intervention rate*. To investigate how this rate impacts the performance, we vary the entropy threshold  $\tau$  for GlimpRouter and the verification threshold for SpecReason. By varying these thresholds, we modulate the proportion of steps processed by the large model. Figure 4 illustrates the accuracy-latency trade-off on multiple benchmarks. The curve of GlimpRouter (red) lies strictly above and to the left of the SpecReason baseline (blue), establishing a superior Pareto frontier. Detailed numerical results are provided in Appendix C.

**Impact of Metric Choice.** To empirically validate the effectiveness of our  $\mathbf{H}_{\text{init}}$  metric, we conducted an ablation study comparing it against two widely used uncertainty metrics: Step-wise Entropy ( $\mathbf{H}_{\text{step}}$ ) and Step-wise Perplexity ( $\mathbf{PPL}_{\text{step}}$ ). Table 2 presents the comparative results on the AIME25 benchmark, while the extended results are detailed in Appendix D. GlimpRouter outperforms both step-wise variants by a significant margin, achieving a relative accuracy gain of **10.7%** over  $\mathbf{H}_{\text{step}}$  and **8.8%** over  $\mathbf{PPL}_{\text{step}}$ . This result corroborates our *Signal Dilution* hypothesis (Section 2.2). Beyond accuracy,  $\mathbf{H}_{\text{init}}$  offers a fundamental advantage in latency (163s vs. 178s / 181s). Implementing routing via step-wise metrics necessitates a “Generate-then-Measure” paradigm, where the initial generation becomes a sunk cost if the step is subsequently routed to  $M_L$ . Conversely,  $\mathbf{H}_{\text{init}}$  operates on a “Probe-then-Dispatch” basis, eliminating the overhead of generating invalid draft steps.

**Orthogonal Speedup with Speculative Decoding.** To demonstrate the versatility of our framework, we evaluate the compatibility of GlimpRouter with

Variants	Acc $\uparrow$	Lat $\downarrow$
<b>GlimpRouter</b>	<b>51.67</b>	<b>163</b>
w/ step-wise entropy	46.67	178
w/ step-wise perplexity	47.50	181

Table 2: Ablation study of different metrics on AIME25. We report accuracy (Acc) and average generation latency (Lat) measured in seconds.

**Speculative Decoding**, a token-level acceleration technique. Table 3 presents the performance metrics when integrating Speculative Decoding into three different inference paradigms: standalone LLM, SpecReason, and GlimpRouter. As shown in Table 3, integrating Speculative Decoding consistently reduces latency across all methods while maintaining comparable accuracy. Crucially, the combination of **GlimpRouter + Speculative Decoding** achieves the lowest end-to-end latency among all configurations. (1) **Global Synergy**: GlimpRouter optimizes the coarse-grained logical flow by routing easy steps to the small model, reducing the total number of calls to the expensive large model. (2) **Local Synergy**: For the difficult steps that are processed by LLM, Speculative Decoding optimizes the fine-grained token generation, mitigating the high per-token cost of the large model. By attacking the efficiency bottleneck from both step-level routing and token-level execution, our framework achieves a compound speedup that surpasses either technique applied in isolation. Additional results on other benchmarks are available in Appendix E.

Method	AIME25		LCBv6	
	Acc $\uparrow$	Lat $\downarrow$	Acc $\uparrow$	Lat $\downarrow$
LLM only	46.67	220	46.86	214
+ Speculative Decoding	45.83	149	46.29	166
SpecReason	49.17	169	47.57	189
+ Speculative Decoding	49.17	140	47.14	154
GlimpRouter	51.67	163	48.29	160
+ Speculative Decoding	51.67	130	48.00	137

Table 3: Evaluation of orthogonality with Speculative Decoding on AIME25 and LCBv6. We report accuracy (Acc) and average generation latency (Lat) measured in seconds.

## 5 Related Work

**Collaborative Inference.** Collaborative inference has emerged as a promising paradigm for

optimizing the efficiency-performance trade-off by leveraging models of varying capacities. Existing approaches generally operate across three interaction granularities: query-level routing (Chen et al., 2023b; Ding et al., 2024; Ong et al., 2024), step-level collaboration (Shi et al., 2025; Pan et al., 2025; Liao et al., 2025), and token-level speculation (Leviathan et al., 2023; Chen et al., 2023a; Cai et al., 2024; Li et al., 2024). Our GlimpRouter distinguishes itself by proposing a training-free, step-level “Probe-then-Dispatch” mechanism based on initial token entropy, which effectively eliminates the sunk costs associated with post-hoc verification.

**Efficient Reasoning.** LRMs such as DeepSeek-R1 (Guo et al., 2025) and OpenAI o1/o3 (Jaech et al., 2024; OpenAI, 2025) demonstrate that scaling test-time compute via Chain-of-Thought (Wei et al., 2022) reasoning significantly enhances reasoning capabilities, albeit at the cost of prohibitive latency. To mitigate this bottleneck, recent research explores dynamic offloading computation to smaller models (Chen et al., 2025b; Wang et al., 2025d; Qu et al., 2025). At the query and token levels, methods utilize trained difficulty predictors (Damani et al., 2024) or trained routers (Fu et al., 2025). Most pertinent to logical deduction is step-level collaboration. Existing methods range from training-based reward guidance (RSD) (Liao et al., 2025) to training-free paradigms relying on multi-path selection (SpecCoT) (Shi et al., 2025) or post-hoc verification (SpecReason) (Pan et al., 2025). Unlike these methods constrained by redundant generation or heavy verification overheads, GlimpRouter achieves efficient orchestration via initial token probing.

## 6 Conclusion

In this work, we addressed the critical latency bottleneck of LRMs by proposing GlimpRouter. This training-free, step-wise collaborative inference framework orchestrates models of varying capacities. We introduce the “Probe-then-Dispatch” mechanism based on initial token entropy. This approach allows the system to anticipate the step difficulty with negligible overhead. Extensive experiments on multiple benchmarks demonstrate that GlimpRouter establishes a superior Pareto frontier. We hope this work enables efficient reasoning and stimulates research on dynamic computation allocation.

## 626 Limitations

627 Despite the efficiency gains demonstrated by  
628 GlimpRouter, we acknowledge several limitations.  
629 First, our routing mechanism relies on a static en-  
630 tropy threshold. While initial token entropy pro-  
631 vides a more continuous and granular signal com-  
632 pared to discrete metrics like LLM-as-a-Judge, a  
633 fixed global threshold may not adapt optimally to  
634 the varying difficulty distributions across diverse  
635 domains or specific query types. Future work could  
636 explore adaptive or instance-aware thresholding  
637 mechanisms to further refine the efficiency. Sec-  
638 ond, the step-level decomposition in our frame-  
639 work relies on explicit structural delimiters (specif-  
640 ically, double newline characters). Although this  
641 formatting pattern is prevalent in Large Reasoning  
642 Models, such as the DeepSeek-R1 and Qwen fami-  
643 lies, this heuristic dependence may limit the frame-  
644 work’s direct applicability to models that gener-  
645 ate unstructured Chain-of-Thought sequences. Ex-  
646 ploring semantic-based segmentation strategies re-  
647 mains a valuable direction for future research.

## 648 References

649 Tianle Cai, Yuhong Li, Zhengyang Geng, Hongwu Peng,  
650 Jason D Lee, Deming Chen, and Tri Dao. 2024.  
651 Medusa: Simple llm inference acceleration frame-  
652 work with multiple decoding heads. *arXiv preprint*  
653 *arXiv:2401.10774*.

654 Charlie Chen, Sebastian Borgeaud, Geoffrey Irving,  
655 Jean-Baptiste Lespiau, Laurent Sifre, and John  
656 Jumper. 2023a. Accelerating large language model  
657 decoding with speculative sampling. *arXiv preprint*  
658 *arXiv:2302.01318*.

659 Lingjiao Chen, Matei Zaharia, and James Zou. 2023b.  
660 Frugalgpt: How to use large language models while  
661 reducing cost and improving performance. *arXiv*  
662 *preprint arXiv:2305.05176*.

663 Silin Chen, Shaoxin Lin, Xiaodong Gu, Yuling Shi,  
664 Heng Lian, Longfei Yun, Dong Chen, Weiguo Sun,  
665 Lin Cao, and Qianxiang Wang. 2025a. Swe-exp:  
666 Experience-driven software issue resolution. *arXiv*  
667 *preprint arXiv:2507.23361*.

668 Yi Chen, JiaHao Zhao, and HaoHao Han. 2025b.  
669 A survey on collaborative mechanisms between  
670 large and small language models. *arXiv preprint*  
671 *arXiv:2505.07460*.

672 Yingqian Cui, Pengfei He, Jingying Zeng, Hui Liu,  
673 Xianfeng Tang, Zhenwei Dai, Yan Han, Chen Luo,  
674 Jing Huang, Zhen Li, and 1 others. 2025. Stepwise  
675 perplexity-guided refinement for efficient chain-of-  
676 thought reasoning in large language models. *arXiv*  
677 *preprint arXiv:2502.13260*.

Mehul Damani, Idan Shenfeld, Andi Peng, Andreea  
678 Bobu, and Jacob Andreas. 2024. Learning how hard  
679 to think: Input-adaptive allocation of lm computation.  
680 *arXiv preprint arXiv:2410.04707*. 681

Dujian Ding, Ankur Mallick, Chi Wang, Robert Sim,  
682 Subhabrata Mukherjee, Victor Ruhle, Laks VS Laksh-  
683 manan, and Ahmed Hassan Awadallah. 2024. Hybrid  
684 llm: Cost-efficient and quality-aware query routing.  
685 *arXiv preprint arXiv:2404.14618*. 686

Tianyu Fu, Yi Ge, Yichen You, Enshu Liu, Zhihang  
687 Yuan, Guohao Dai, Shengen Yan, Huazhong Yang,  
688 and Yu Wang. 2025. R2r: Efficiently navigating  
689 divergent reasoning paths with small-large model  
690 token routing. *arXiv preprint arXiv:2505.21600*. 691

Daya Guo, Dejian Yang, Haowei Zhang, Junxiao  
692 Song, Ruoyu Zhang, Runxin Xu, Qihao Zhu, Shi-  
693 rong Ma, Peiyi Wang, Xiao Bi, and 1 others. 2025.  
694 Deepseek-r1: Incentivizing reasoning capability in  
695 llms via reinforcement learning. *arXiv preprint*  
696 *arXiv:2501.12948*. 697

Minghao Hu, Junzhe Wang, Weisen Zhao, Qiang Zeng,  
698 and Lannan Luo. 2025. Flowmaltrans: Unsuper-  
699 vised binary code translation for malware detec-  
700 tion using flow-adapter architecture. *arXiv preprint*  
701 *arXiv:2508.20212*. 702

Aaron Jaech, Adam Kalai, Adam Lerer, Adam Richard-  
703 son, Ahmed El-Kishky, Aiden Low, Alec Helyar,  
704 Aleksander Madry, Alex Beutel, Alex Carney, and 1  
705 others. 2024. Openai o1 system card. *arXiv preprint*  
706 *arXiv:2412.16720*. 707

Naman Jain, King Han, Alex Gu, Wen-Ding Li, Fanjia  
708 Yan, Tianjun Zhang, Sida Wang, Armando Solar-  
709 Lezama, Koushik Sen, and Ion Stoica. 2024. Live-  
710 codebench: Holistic and contamination free eval-  
711 uation of large language models for code. *arXiv*  
712 *preprint arXiv:2403.07974*. 713

Lorenz Kuhn, Yarin Gal, and Sebastian Farquhar. 2023.  
714 Semantic uncertainty: Linguistic invariances for un-  
715 certainty estimation in natural language generation.  
716 *arXiv preprint arXiv:2302.09664*. 717

Woosuk Kwon, Zhuohan Li, Siyuan Zhuang, Ying  
718 Sheng, Lianmin Zheng, Cody Hao Yu, Joseph E.  
719 Gonzalez, Hao Zhang, and Ion Stoica. 2023. Effi-  
720 cient memory management for large language model  
721 serving with pagedattention. In *Proceedings of the*  
722 *ACM SIGOPS 29th Symposium on Operating Systems*  
723 *Principles*. 724

Yaniv Leviathan, Matan Kalman, and Yossi Matias.  
725 2023. Fast inference from transformers via spec-  
726 ulative decoding. In *International Conference on*  
727 *Machine Learning*, pages 19274–19286. PMLR. 728

Han Li, Yuling Shi, Shaoxin Lin, Xiaodong Gu, Heng  
729 Lian, Xin Wang, Yantao Jia, Tao Huang, and Qianxi-  
730 ang Wang. 2025. Swe-debate: Competitive multi-  
731 agent debate for software issue resolution. *arXiv*  
732 *preprint arXiv:2507.23348*. 733

734	Yuhui Li, Fangyun Wei, Chao Zhang, and Hongyang Zhang. 2024. Eagle: Speculative sampling requires rethinking feature uncertainty. <i>arXiv preprint arXiv:2401.15077</i> .	790
735		791
736		792
737		793
738	Baohao Liao, Yuhui Xu, Hanze Dong, Junnan Li, Christof Monz, Silvio Savarese, Doyen Sahoo, and Caiming Xiong. 2025. Reward-guided speculative decoding for efficient llm reasoning. In <i>Forty-second International Conference on Machine Learning</i> .	794
739		795
740		796
741		797
742		798
743	Chin-Yew Lin and Franz Josef Och. 2004. Orange: a method for evaluating automatic evaluation metrics for machine translation. In <i>COLING 2004: Proceedings of the 20th International Conference on Computational Linguistics</i> , pages 501–507.	799
744		800
745		
746		
747		
748	Andrey Malinin and Mark Gales. 2020. Uncertainty estimation in autoregressive structured prediction. <i>arXiv preprint arXiv:2002.07650</i> .	801
749		802
750		803
751	Isaac Ong, Amjad Almahairi, Vincent Wu, Wei-Lin Chiang, Tianhao Wu, Joseph E Gonzalez, M Waleed Kadous, and Ion Stoica. 2024. Routellm: Learning to route llms with preference data. <i>arXiv preprint arXiv:2406.18665</i> .	804
752		805
753		806
754		
755		
756	OpenAI. 2025. <a href="#">Openai o3 and o4-mini system card</a> .	807
757	Rui Pan, Yinwei Dai, Zhihao Zhang, Gabriele Oliaro, Zhihao Jia, and Ravi Neeravali. 2025. Specreason: Fast and accurate inference-time compute via speculative reasoning. <i>arXiv preprint arXiv:2504.07891</i> .	808
758		809
759		810
760		811
761	Xiaoye Qu, Yafu Li, Zhaochen Su, Weigao Sun, Jianhao Yan, Dongrui Liu, Ganqu Cui, Daizong Liu, Shuxian Liang, Junxian He, and 1 others. 2025. A survey of efficient reasoning for large reasoning models: Language, multimodality, and beyond. <i>arXiv preprint arXiv:2503.21614</i> .	812
762		813
763		814
764		815
765		816
766		817
767	Nils Reimers and Iryna Gurevych. 2019. <a href="#">Sentence-bert: Sentence embeddings using siamese bert-networks</a> . In <i>Proceedings of the 2019 Conference on Empirical Methods in Natural Language Processing</i> . Association for Computational Linguistics.	818
768		819
769		820
770		821
771		
772	David Rein, Betty Li Hou, Asa Cooper Stickland, Jackson Petty, Richard Yuanzhe Pang, Julien Dirani, Julian Michael, and Samuel R Bowman. 2024. Gpqa: A graduate-level google-proof q&a benchmark. In <i>First Conference on Language Modeling</i> .	822
773		823
774		824
775		825
776		826
777	Claude E Shannon. 1948. A mathematical theory of communication. <i>The Bell system technical journal</i> , 27(3):379–423.	827
778		828
779		829
780	Jianshu She, Zhuohao Li, Zhemin Huang, Qi Li, Peiran Xu, Haonan Li, and Qirong Ho. 2025. Hawkeye: Model collaboration for efficient reasoning. In <i>Second Conference on Language Modeling</i> .	830
781		
782		
783		
784	Junhan Shi, Yijia Zhu, Zhenning Shi, Dan Zhao, Qing Li, and Yong Jiang. 2025. Speccot: Accelerating chain-of-thought reasoning through speculative exploration. In <i>Findings of the Association for Computational Linguistics: EMNLP 2025</i> , pages 24405–24415.	831
785		832
786		833
787		834
788		835
789		
	Qiuchen Wang, Ruixue Ding, Zehui Chen, Weiqi Wu, Shihang Wang, Pengjun Xie, and Feng Zhao. 2025a. Vidorag: Visual document retrieval-augmented generation via dynamic iterative reasoning agents. <i>arXiv preprint arXiv:2502.18017</i> .	836
		837
		838
		839
	Qiuchen Wang, Ruixue Ding, Yu Zeng, Zehui Chen, Lin Chen, Shihang Wang, Pengjun Xie, Fei Huang, and Feng Zhao. 2025b. Vrag-rl: Empower vision-perception-based rag for visually rich information understanding via iterative reasoning with reinforcement learning. <i>arXiv preprint arXiv:2505.22019</i> .	840
		841
		842
		843
		844
	Shenzhi Wang, Le Yu, Chang Gao, Chujie Zheng, Shixuan Liu, Rui Lu, Kai Dang, Xionghui Chen, Jianxin Yang, Zhenru Zhang, and 1 others. 2025c. Beyond the 80/20 rule: High-entropy minority tokens drive effective reinforcement learning for llm reasoning. <i>arXiv preprint arXiv:2506.01939</i> .	
	Xinyuan Wang, Yanchi Liu, Wei Cheng, Xujiang Zhao, Zhengzhang Chen, Wenchao Yu, Yanjie Fu, and Haifeng Chen. 2025d. Mixllm: Dynamic routing in mixed large language models. <i>arXiv preprint arXiv:2502.18482</i> .	
	Jason Wei, Xuezhi Wang, Dale Schuurmans, Maarten Bosma, Fei Xia, Ed Chi, Quoc V Le, Denny Zhou, and 1 others. 2022. Chain-of-thought prompting elicits reasoning in large language models. <i>Advances in neural information processing systems</i> , 35:24824–24837.	
	Zilin Xiao, Jaywon Koo, Siru Ouyang, Jefferson Hernandez, Yu Meng, and Vicente Ordonez. 2025. Prox-thinker: Test-time guidance through small visual reasoners. <i>arXiv preprint arXiv:2505.24872</i> .	
	An Yang, Anfeng Li, Baosong Yang, Beichen Zhang, Binyuan Hui, Bo Zheng, Bowen Yu, Chang Gao, Chengen Huang, Chenxu Lv, and 1 others. 2025a. Qwen3 technical report. <i>arXiv preprint arXiv:2505.09388</i> .	
	Wang Yang, Xiang Yue, Vipin Chaudhary, and Xiaotian Han. 2025b. Speculative thinking: Enhancing small-model reasoning with large model guidance at inference time. <i>arXiv preprint arXiv:2504.12329</i> .	
	Xinwei Yang, Zhaofeng Liu, Chen Huang, Jiashuai Zhang, Tong Zhang, Yifan Zhang, and Wenqiang Lei. 2025c. Elaboration: A comprehensive benchmark on human-llm competitive programming. <i>arXiv preprint arXiv:2505.16667</i> .	
	Qingcheng Zeng, Weihao Xuan, Leyang Cui, and Rob Voigt. 2025a. Thinking out loud: Do reasoning models know when they’re right? <i>arXiv preprint arXiv:2504.06564</i> .	
	Wenhao Zeng, Yaoning Wang, Chao Hu, Yuling Shi, Chengcheng Wan, Hongyu Zhang, and Xiaodong Gu. 2025b. Pruning the unsurprising: Efficient code reasoning via first-token surprisal. <i>arXiv preprint arXiv:2508.05988</i> .	

Jinghan Zhang, Xiting Wang, Fengran Mo, Yeyang Zhou, Wanfu Gao, and Kunpeng Liu. 2025. Entropy-based exploration conduction for multi-step reasoning. *arXiv preprint arXiv:2503.15848*.

Lianmin Zheng, Liangsheng Yin, Zhiqiang Xie, Chuyue Livia Sun, Jeff Huang, Cody Hao Yu, Shiyi Cao, Christos Kozyrakis, Ion Stoica, Joseph E Gonzalez, and 1 others. 2024. Sglang: Efficient execution of structured language model programs. *Advances in neural information processing systems*, 37:62557–62583.

## A Pseudocode of GlimpRouter

The pseudocode of GlimpRouter is provided in Algorithm 1. Given an input question, the system operates in a step-wise manner. At the onset of each step, instead of blindly generating the full content, GlimpRouter employs  $M_S$  to “glimpse” the first token, yielding an entropy  $\mathbf{H}_{\text{init}}$  that quantizes the difficulty of the upcoming step: If  $\mathbf{H}_{\text{init}}$  falls below a threshold, the step is deemed routine, and the small model is responsible for continuing the generation. Otherwise, the step signals a cognitive pivot, and the context is handed over to a large model for high-quality generation.

---

### Algorithm 1 Step-wise Collaborative Inference via GlimpRouter

---

```

1: Inputs: question  $q$ , large model  $M_L$ , small model  $M_S$ , entropy threshold  $\tau$ 
2: Output: a composite reasoning chain  $\hat{T}$ 
3:  $\hat{T} \leftarrow \emptyset$  // Initialize the reasoning chain
4:  $k \leftarrow 1$ 
5: while not finished do
6:    $\mathbf{c}_k = \text{CONCAT}(q, \hat{T})$  // Construct the current context by concatenating question and historical steps
7:    $P_{\text{init}} = M_S(\mathbf{c}_k)$  // Compute the first-token distribution using the small model
8:   Calculate the initial token entropy  $\mathbf{H}_{\text{init}}(s_k)$ 
9:   if  $\mathbf{H}_{\text{init}}(s_k) > \tau$  then
10:     $\hat{s}_k \leftarrow M_L(\mathbf{c}_k)$  // Generate  $\hat{s}_k$  using the large model
11:   else
12:     $\hat{s}_k \leftarrow M_S(\mathbf{c}_k)$  // Generate  $\hat{s}_k$  using the small model
13:   end if
14:    $\hat{T} = \text{CONCAT}(\hat{T}, \hat{s}_k)$  // Append the generated step to the reasoning chain
15:    $k \leftarrow k + 1$ 
16: end while
17: return  $\hat{T}$ 

```

---

## B Scalability across Architectural Pairings

To verify the universality of GlimpRouter beyond specific small models (e.g., Qwen3-4B), we ex-

tend our evaluation to a homogeneous model family setting. Specifically, we employ DeepSeek-R1-Distill-Qwen-1.5B as the small model (SLM) and DeepSeek-R1-Distill-Qwen-32B as the large model (LLM).

Table 4 presents the comparative results on the AIME, GPQA-Diamond, and LiveCodeBench benchmarks. Consistent with the observations in our main experiments (Section 4.2), GlimpRouter continues to exhibit a superior efficiency-performance trade-off compared to baselines. Despite the change in the small model, GlimpRouter maintains its advantage over reactive baselines such as RSD, SpecReason, and SpecCoT. While baselines incur significant latency overhead due to full-step generation and verification, GlimpRouter effectively leverages  $\mathbf{H}_{\text{init}}$  to route simpler steps to DeepSeek-R1-Distill-Qwen-1.5B preemptively. The success of GlimpRouter in this DeepSeek-R1-Distill-Qwen-1.5B + DeepSeek-R1-Distill-Qwen-32B setting underscores the robustness of the “Probe-then-Dispatch” mechanism. It suggests that the correlation between the initial token’s entropy and step-level difficulty is not an artifact of specific datasets or model families, but rather an intrinsic property of large reasoning models.

## C Detailed Sensitivity Analysis of Collaboration Thresholds

In this section, we present the comprehensive numerical results that underpin the sensitivity analysis discussed in Section 4.3. We examine the impact of varying the thresholds on the intervention rate, defined as the percentage of reasoning steps generated by the large model ( $M_L$ ), and the resulting efficiency-performance trade-offs. We evaluate two distinct routing mechanisms: We sweep the Initial Token Entropy ( $\mathbf{H}_{\text{init}}$ ) threshold  $\tau \in \{0.01, 0.1, 0.6, 0.9, 1.8\}$ . A lower  $\tau$  makes the system more cautious, triggering  $M_L$  more frequently (Higher Intervention). We vary the verification confidence threshold  $\sigma \in \{6, 7, 8, 9\}$  of SpecReason. A stricter threshold leads to higher rejection rates, forcing  $M_L$  to regenerate steps more frequently (Higher Intervention).

Table 5 details the performance metrics on the AIME and LiveCodeBench benchmarks. A critical observation is the scaling behavior of latency with respect to the intervention rate. For GlimpRouter, latency increases linearly and modestly as the in-

Method	AIME24		AIME25		GPQA		LCBv5		LCBv6	
	Acc $\uparrow$	Lat $\downarrow$	Acc $\uparrow$	Lat $\downarrow$	Acc $\uparrow$	Lat $\downarrow$	Acc $\uparrow$	Lat $\downarrow$	Acc $\uparrow$	Lat $\downarrow$
SLM only	25.83	60	26.67	57	15.91	37	15.12	66	20.29	62
LLM only	57.50	197	46.67	220	61.62	176	52.40	219	46.86	214
Random	43.33	127	28.33	135	46.46	88	37.13	142	33.71	138
RSD	46.67	162	35.83	173	49.90	123	41.32	198	37.71	197
SpecCoT	50.00	158	30.83	168	51.01	121	37.96	193	37.03	184
SpecReason	45.83	152	31.67	171	53.41	159	38.08	192	38.26	190
GlimpRouter	<b>51.67</b>	145	<b>39.17</b>	166	<b>54.04</b>	117	<b>45.66</b>	189	<b>43.57</b>	182

Table 4: Performance comparison with DeepSeek-R1-Distill-Qwen-1.5B as SLM and DeepSeek-R1-Distill-Qwen-32B as LLM. Acc and Lat represent Accuracy (Pass@1, %) and Average Latency (s), respectively. The best performance is highlighted in bold.

Method	Thr.	AIME24			AIME25			LCBv5			LCBv6		
		Acc $\uparrow$	Lat $\downarrow$	Rate	Acc $\uparrow$	Lat $\downarrow$	Rate	Acc $\uparrow$	Lat $\downarrow$	Rate	Acc $\uparrow$	Lat $\downarrow$	Rate
<b>SLM only</b>	-	48.33	99	0	45.00	105	0	47.90	100	0	43.71	94	0
<b>LLM only</b>	-	57.50	197	100	46.67	220	100	52.40	219	100	46.86	214	100
<b>SpecReason</b>	$\sigma = 6$	50.00	128	2	45.00	138	2	50.89	130	13	45.80	139	15
	$\sigma = 7$	53.33	146	5	48.33	151	4	52.69	141	17	46.86	144	17
	$\sigma = 8$	57.50	158	14	49.17	169	12	53.59	185	32	47.57	189	37
	$\sigma = 9$	61.67	220	48	51.67	249	51	54.20	250	87	48.00	260	87
<b>GlimpRouter</b>	$\tau = 1.8$	51.67	128	2	45.83	138	2	51.60	110	2	47.43	111	2
	$\tau = 0.9$	60.83	143	26	51.67	163	27	54.64	160	37	48.29	160	37
	$\tau = 0.6$	61.67	160	44	55.00	181	45	55.30	179	60	48.95	183	65
	$\tau = 0.1$	63.33	181	76	55.67	205	76	55.50	221	84	49.10	221	88
	$\tau = 0.01$	63.67	194	85	55.83	212	83	55.50	227	89	49.15	227	91

Table 5: Detailed sensitivity analysis of routing thresholds across different benchmarks. **Thr.**: Routing threshold ( $\tau$  for GlimpRouter,  $\sigma$  for SpecReason). **Acc.**: Pass@1 Accuracy. **Lat.**: Average Latency. **Rate.**: Intervention Rate, the percentage of steps generated by the large model ( $M_L$ ).

intervention rate rises. This is because the overhead of checking the first token is negligible; the latency cost is purely the difference between  $M_L$  and  $M_S$  generation speeds. In stark contrast, SpecReason exhibits a super-linear latency spike as the intervention rate increases. Taking AIME25 as an example, at an intervention rate of approximately  $\sim 50\%$ , the latency of SpecReason is significantly higher than that of GlimpRouter. This confirms the ‘‘Sunk Cost’’ hypothesis: SpecReason must waste time generating a full draft by  $M_S$  before  $M_L$  can intervene, whereas GlimpRouter proactively dispatches the task, eliminating redundant computation. Furthermore, comparing iso-accuracy configurations (e.g., GlimpRouter with  $\tau = 0.9$  vs. SpecReason with  $\sigma = 9$ , both achieving 51.67% on AIME25), our

method consistently achieves lower latency. This numerical evidence substantiates the visual trend observed in the Pareto frontier (Figure 4), demonstrating that  $\mathbf{H}_{\text{init}}$  is more efficient than post-hoc verification.

## D Extended Analysis of Metric Choice

In Section 4.3, we demonstrate the superiority of the initial token entropy ( $\mathbf{H}_{\text{init}}$ ) on the AIME25 benchmark. We extend the ablation study to include AIME24, AIME25, LiveCodeBench v5, and LiveCodeBench v6. Table 6 presents the comprehensive results comparing GlimpRouter against Step-wise Entropy ( $\mathbf{H}_{\text{step}}$ ) and Step-wise Perplexity ( $\mathbf{PPL}_{\text{step}}$ ).

Across all four benchmarks, GlimpRouter em-

Variants	AIME24		AIME25		LCBv5		LCBv6	
	Acc ↑	Lat ↓	Acc ↑	Lat ↓	Acc ↑	Lat ↓	Acc ↑	Lat ↓
<b>GlimpRouter</b>	<b>60.83</b>	<b>143</b>	<b>51.67</b>	<b>163</b>	<b>54.64</b>	<b>160</b>	<b>48.29</b>	<b>160</b>
w/ step-wise entropy	58.33	163	46.67	178	53.44	185	47.29	194
w/ step-wise perplexity	59.17	159	47.50	181	53.29	181	47.43	194

Table 6: Comprehensive ablation studies of metrics on four benchmarks. We report accuracy (Acc) and average generation latency (Lat) measured in seconds.

Method	AIME24		AIME25		LCBv5		LCBv6	
	Acc ↑	Lat ↓	Acc ↑	Lat ↓	Acc ↑	Lat ↓	Acc ↑	Lat ↓
LLM only	57.50	197	46.67	220	52.40	219	46.86	214
+ Speculative Decoding	56.67	139	45.83	149	51.80	165	46.29	166
SpecReason	57.50	158	49.17	169	53.59	185	47.57	189
+ Speculative Decoding	57.50	133	49.17	140	53.29	151	47.14	154
GlimpRouter	60.83	143	51.67	163	54.64	160	48.29	160
+ Speculative Decoding	60.00	116	51.67	130	54.34	134	48.00	137

Table 7: Comprehensive evaluation of orthogonal speedup with Speculative Decoding across four benchmarks. We report accuracy (Acc) and average generation latency (Lat) measured in seconds. Rows highlighted in gray indicate the integration of token-level speculative decoding.

954 ploying  $\mathbf{H}_{\text{init}}$  consistently achieves the highest ac- 979  
955 curacy. This universal superiority strongly supports 980  
956 the **Signal Dilution** hypothesis. Step-wise metrics, 981  
957 by averaging uncertainty over the entire sequence 982  
958 length  $L$ , allow high-confidence syntactic tokens to 983  
959 obscure the signals from critical reasoning nodes. 984  
960 In contrast,  $\mathbf{H}_{\text{init}}$  focuses exclusively on the cog- 985  
961 nitive pivot (the initial token), providing a sharper, 986  
962 undiluted signal that effectively distinguishes be- 987  
963 tween routine steps and complex logical bifurca- 988  
964 tions. Regarding efficiency, the results highlight 989  
965 a fundamental structural advantage of our method. 990  
966 On every benchmark, the step-wise metrics incur 991  
967 higher latency than GlimpRouter, despite operating 992  
968 at similar intervention rates. This is because step- 993  
969 wise metrics operate on a “Generate-then-Measure” 994  
970 paradigm: the small model must fully generate a 995  
971 step before its difficulty can be assessed. If the step 996  
972 is subsequently rejected and routed to the large 997  
973 model, the initial generation becomes a sunk cost. 998  
974 GlimpRouter, leveraging the “Probe-then-Dispatch” 999  
975 mechanism, assesses difficulty before generation. 1000  
976 This proactive routing eliminates invalid drafting, 1001  
977 ensuring that computational resources are allocated 1002  
978 with maximal efficiency. 1003  
1004

## E Extended Analysis of Orthogonality with Speculative Decoding

In Section 4.3, we demonstrated the compatibility of GlimpRouter with Speculative Decoding on specific benchmarks. To verify that this compound speedup is a universal property of our framework, we extend the evaluation to the full suite of benchmarks: AIME24, AIME25, LiveCodeBench v5, and LiveCodeBench v6. Table 7 details the performance metrics for three inference paradigms (Standalone LLM, SpecReason, and GlimpRouter), both with and without Token-level Speculative Decoding.

As evidenced in Table 7, integrating Speculative Decoding yields consistent latency reductions across all methods and benchmarks. For the standalone LLM, latency drops by approximately **22%–32%**. For the collaborative methods (SpecReason and GlimpRouter), the token-level acceleration further compresses the execution time of the large model’s generation phases. Importantly, this speedup is achieved with negligible impact on reasoning accuracy. Crucially, the combination of **GlimpRouter + Speculative Decoding** achieves the lowest end-to-end latency across all experimental configurations. Even when the strong

baseline, SpecReason, is accelerated by Speculative Decoding, it remains consistently slower than our enhanced framework (e.g., 140s vs. 130s on AIME25). This gap highlights a fundamental architectural distinction: Token-level speculation can only accelerate the generation process; it cannot recover the sunk costs of invalid steps discarded during reactive verification. SpecReason still pays the penalty for generating and rejecting full steps. In contrast, GlimpRouter leverages  $H_{\text{init}}$  to proactively route steps, minimizing the number of tokens that need to be generated in the first place. When combined with Speculative Decoding, which accelerates the tokens that must be generated by  $M_L$ , we achieve a multiplicative effect on efficiency. This confirms that GlimpRouter serves as an ideal **Global Planner**, perfectly complementing **Local Executors** like Speculative Decoding to establish a new state-of-the-art Pareto frontier.

## F Case Studies

### F.1 Case Study 1: Correlation between Initial Token Entropy ( $H_{\text{init}}$ ) and Reasoning Difficulty

We provide a concrete example to show the correlation between  $H_{\text{init}}$  and reasoning difficulty. The case visualizes how GlimpRouter dynamically allocates computational resources based on the cognitive load of each step. The case below illustrates a representative trajectory from the AIME benchmark. We observe a clear dichotomy in  $H_{\text{init}}$  values corresponding to the nature of the reasoning steps:

- **Low  $H_{\text{init}}$  (Routine Execution):** Steps 1-2 and 5-12 exhibit extremely low  $H_{\text{init}}$  values (e.g., 0.0046, 0.0008). These steps involve factual restatements or mechanical algorithmic operations (e.g., recursive division by 2). The small model ( $M_S$ ) demonstrates high confidence and generates these tokens accurately, validating our “Delegate” strategy.
- **High  $H_{\text{init}}$  (Cognitive Bifurcation):** A critical spike in entropy occurs at the onset of Step 3 ( $H_{\text{init}}$ : 1.8985). Here, the reasoning process transitions from problem setup to solution planning. The small model’s draft (starting with “Maybe”) reflects uncertainty in selecting the counting method.

### A Case of Correlation between Initial Token Entropy ( $H_{\text{init}}$ ) and Reasoning Difficulty

#### Question:

Alice chooses a set  $A$  of positive integers. Bob lists all finite nonempty sets  $B$  whose maximum is in  $A$ . Bob’s list has 2024 sets. Find the sum of the elements of  $A$ .

#### Reasoning Trace via GlimpRouter:

##### Step 1 [SLM] ( $H_{\text{init}}$ : 0.2369)

First, Alice chooses a set  $A$ , and Bob lists all nonempty sets  $B$  whose maximum is in  $A$ ; there are 2024 such sets.

##### Step 2 [SLM] ( $H_{\text{init}}$ : 0.3485)

If  $A = \{2\}$ , then  $B$  can be  $\{2\}$  or  $\{1, 2\}$ , giving  $2^{2-1} = 2$  sets. Generally, the number of sets corresponds to a sum of powers of 2.

##### Step 3 (Critical Pivot)

**Content ( $M_S$ ):** “Maybe I can try to find...” ( $H_{\text{init}}$ : 1.8985 >  $\tau$ )

↪ **Action: Intervene ( $M_L$ )**

**Content ( $M_L$ ):** The most efficient way is to divide 2024 by 2 repeatedly to find its binary representation directly.

##### Step 4 [SLM] ( $H_{\text{init}}$ : 0.0046)

Compute  $2024/2 = 1012$ , remainder 0.

##### Step 5 [SLM] ( $H_{\text{init}}$ : 0.0008)

Then  $1012/2 = 506$ , remainder 0.

##### Step 6 [SLM] ( $H_{\text{init}}$ : 0.0102)

Next  $506/2 = 253$ , remainder 0.

##### Steps 7-10 [SLM] ( $H_{\text{init}}$ values: 0.0055, 0.0032, 0.0041)

[...Routine division steps:  $253 \rightarrow 126 \rightarrow 63 \rightarrow 31...$ ]

##### Step 11 [SLM] ( $H_{\text{init}}$ : 0.1205)

So the binary representation is  $1111101000_2$ . This corresponds to powers  $2^{10}, \dots, 2^3$ . Since the term is  $2^{a-1}$ , the elements are  $a \in \{11, 10, 9, 8, 7, 6, 4\}$ .

##### Step 12 [SLM] ( $H_{\text{init}}$ : 0.0020)

Finally, the sum is  $11 + 10 + 9 + 8 + 7 + 6 + 4 = \boxed{55}$ .

### F.2 Case Study 2: Self-Correction Mechanism in LRMs

The case below demonstrates the system’s ability to detect and correct potential logical errors during the reasoning process. In combinatorics problems involving grid paths, an accurate definition of geometric properties is a prerequisite for calculation.

- **Logical Instability:** In Step 3, the small model establishes the relationship between “direction changes” and “path segments”. It produces content containing a factual error: equating four direction changes to *four* segments (the correct number is  $4 + 1 = 5$ ).
- **Correction via Intervention:** Upon triggering the high-entropy threshold in Step 4, GlimpRouter invokes the large model ( $M_L$ ). Crucially,  $M_L$  does not merely complete the

1069 SLM’s erroneous sentence. Instead, it re-  
 1070 evaluates the context and generates a correct  
 1071 premise: “that means it has five straight seg-  
 1072 ments.”

- 1073 • **Outcome:** By correcting the hallucinated step  
 1074 and injecting the correct geometric reasoning,  
 1075  $M_L$  steers the trajectory back to a valid path.  
 1076 Subsequently,  $M_S$  successfully performs the  
 1077 routine combinatorial calculations (Steps 5-6)  
 1078 based on the corrected logic.

### A Case of the Self-correction Mechanism in LRMs

**Question:**

Consider the paths of length 16 that follow the lines from the lower left corner to the upper right corner on an  $8 \times 8$  grid. Find the number of such paths that change direction exactly four times.

**Reasoning Trace via GlimpRouter:**

**Step 1 [SLM] (H<sub>init</sub>: 0.2457)**

So, the problem is about paths on a grid where you start at (0,0) and end at (8,8), moving only right (R) or up (U), each step being a unit move.

**Step 2 [SLM] (H<sub>init</sub>: 0.3914)**

Let me recall that in such grid paths, a path that goes from (0,0) to (8,8) can be represented as a sequence of right (R) and up (U) moves.

**Step 3 [SLM] (Logical Divergence)**

Suppose a path starts... four direction changes mean the path has *four segments*.

**Step 4 [LLM] (Logical Correction)**

Wait, if a path changes direction exactly four times, that means it has *five straight segments*. Because each change of direction adds a new segment. For example, starting with R gives R-U-R-U-R.

**Step 5 [SLM] (H<sub>init</sub>: 0.4949)**

Let me recall that the number of compositions of n into k positive integers is  $C(n-1, k-1)$ . Because it’s equivalent to placing k-1 dividers in the n-1 gaps between n items.

**Step 6 [SLM] (H<sub>init</sub>: 0.2771)**

Therefore, the total number is  $2 \times \left[ \binom{7}{2} \times \binom{7}{1} \right] = 2 \times 21 \times 7 = \boxed{294}$ .

1079